Deep-Sea Research I 55 (2008) 832–846

Contents lists available at ScienceDirect

Deep-Sea Research I

journal homepage: www.elsevier.com/locate/dsri

Chlorophyll maxima and water mass interfaces: Tidally induced dynamics in the Strait of Gibraltar

D. Macías [a,*], L.M. Lubián [b], F. Echevarría [a,c], I.E. Huertas [b], C.M. García [a]

[a] Departamento de Biología, Área de Ecología, Facultad de Ciencias del Mar y Ambientales, Universidad de Cádiz, 11510 Puerto Real, Cádiz, Spain
[b] Instituto de Ciencias Marinas de Andalucía (ICMAN), CSIC, 11510 Puerto Real, Cádiz, Spain
[c] Centro Andaluz de Ciencia y Tecnología Marina (CACYTMAR), 11510 Puerto Real, Cádiz, Spain

ARTICLE INFO

Article history:
Received 24 May 2007
Received in revised form
24 March 2008
Accepted 30 March 2008
Available online 3 April 2008

Keywords:
Strait of Gibraltar
Atlantic jet
Tidal forcing
Deep chlorophyll maximum
Circulation schemes
Interfaces
Vertical structure

ABSTRACT

A conceptual model proposing the distribution and dynamics of water masses and chlorophyll maxima according to tidal cycle is presented for the Strait of Gibraltar. The proposal is based on the analysis of data registered in a section along the strait at different stages of the tidal cycle. Basic water characteristics were established from CTD casts combined with bottle sampling. Composition and nature of the phytoplankton assemblage were studied by analysis of chlorophyll, pulse amplitude modulated fluorometry, flow cytometry and light microscopy analyses. The usual occurrence of deep chlorophyll maximum (DCM) linked to pycnoclines and/or water mass interfaces draws complicate patterns in the Gibraltar region, as three water masses (SAW, MOW and NACW) meet in the upper layers of the water column. The results indicate that the chlorophyll maxima found in the channel of the strait are not homogeneous and could be classified into at least three types: Atlantic maxima, linked to the SAW–NACW interface; suction maxima, present only in the SAW–MOW interface and deep maxima, associated with the transition NACW–MOW on the eastern side of the strait. These chlorophyll maxima are strongly associated with the different water mass interfaces and, even more, to a specific water density following the movement of these water mass interfaces, which is forced mainly by the tidal amplitude in this area. This study also adds new elements supporting the hypothesis that some of the pulsating chlorophyll patches observed in the strait could have a coastal origin, as their characteristics were clearly different from those of other chlorophyll maxima detected in the channel but originating in the open sea.

1. Introduction

One of the most distinct and ubiquitous biological features in the world's ocean is the presence of a deep (or sub-surface) chlorophyll maximum (DCM) associated with discontinuities in the water column, such as the seasonal thermocline or the presence of haloclines, particularly where different water masses meet. This situation is often the case in semi-enclosed basins (such as the Mediterranean or Baltic Sea) and coastal areas where river discharges create intense pycnoclines.

The existence of a DCM, in conjunction with seasonal variations in the depth of the mixed layer, is of crucial importance for explaining the annual cycle of primary production in the open ocean (Gran, 1931; Sverdrup, 1953). Thus, coupled biological–physical studies which focus on the interfaces separating different water masses are of particular relevance, since it is presumably in these areas, characterised by marked gradients, where phytoplankton cells tend to accumulate (Mann and Lazier, 1991; Rodríguez et al., 1998).

Although the mechanism of DCM formation is still under debate, it can be attributed either to an increase in

* Corresponding author. Tel.: +34 956 016025; fax: +34 956 016019.
E-mail address: diego.macias@uca.es (D. Macías).

0967-0637/$ - see front matter © 2008 Elsevier Ltd. All rights reserved.
doi:10.1016/j.dsr.2008.03.008

the cell chlorophyll content due to photoadaptation (Taguchi et al., 1984); to an increase in phytoplankton growth rates due to the existence of a marked nutricline (Jamart et al., 1977; Cullen and Eppley, 1981) or to physical accumulation of phytoplankton cells at interfaces (Herbland and Voituriez, 1979; Longhurst and Harrison, 1989; Margalef, 1978; Ruiz et al., 2004).

The relationship between DCM, water masses and hydrodynamic conditions has been extensively studied both in the Mediterranean basin and in the Gulf of Cadiz, the two oceanographic regions connected by the Strait of Gibraltar. The existence of a DCM in the Mediterranean Sea is of particular relevance; surface waters of this basin are typically very oligotrophic and the development of vertical patterns of chlorophyll distribution is intimately linked both to the hydrographical characteristics at different spatio-temporal scales (Estrada et al., 1999) and the fertilisation mechanisms of the photic layer (Estrada et al., 1993; Morán et al., 2001). Moreover, Mediterranean waters are a mixture of different water masses with specific thermohaline characteristics (Guibout, 1987; La Violette, 1995); hence addressing the importance of interfaces on the development of DCM is of capital importance for the conjunct of this basin.

Phytoplankton biomass accumulation at density singularities (pycnoclines) was recently demonstrated in the Gulf of Cadiz, where chlorophyll maximum were clearly associated with the interface between the Surface Atlantic Waters (SAW) and the North Atlantic Central Waters (NACW) on the 26.6 isopycnal (Navarro et al., 2006). The occurrence of this maximum was explained by the existence of a marked nutricline between both water masses.

In the Strait of Gibraltar, the vertical distribution of DCM is likely to be far more complicated because of the simultaneous presence of different typical water masses (SAW, NACW and Mediterranean Outflowing Water (MOW)), leading to the presence of multiple density interfaces. In addition, due to the complexity of the hydrodynamic processes within the strait, some of these water masses appear intermittently (particularly the less abundant NACW, see Gascard and Richez, 1985; Macías et al., 2006), creating considerable spatial and temporal variations in the position and intensity of interfaces.

The average circulation through the strait can be described as a two-layer inverse-estuarine exchange with a superficial inflow of Atlantic waters and a deep outflow of Mediterranean waters (Armi and Farmer, 1988). Circulation is maintained by the negative hydrological budget of the Mediterranean basin, where evaporation exceeds precipitation plus river discharges (Béthoux, 1979). However, this general scheme undergoes strong modifications that are particularly noticeable at tidal scale (García-Lafuente and Vargas, 2003), as tide-forced flows interact with the sharp topography of the channel of the strait. This interaction generates undulatory features at the Atlantic–Mediterranean Interface (AMI) such as internal bores (Boyce, 1975; Armi and Farmer, 1985) or internal waves (Bruno et al., 2002). These processes can produce vigorous interfacial mixing (Bray et al., 1995; Wesson and Gregg, 1994), changing the properties of the Atlantic jet at it enters the Mediterranean.

Water mass distribution in the Atlantic jet and biological patterns are highly related in this region (Gómez et al., 2001, 2004; Macías et al., 2006), with tidal phase and magnitude (Macías et al., 2006) or wind regime being the principle factors that control the discontinuous (horizontal entrainment) entrance of chlorophyll patches into the Alborán Sea. The vertical distribution of chlorophyll is also expected to be linked to the dynamics of the water masses, which show clear vertical segregation, with SAW at the surface, MOW in the deeper layers and NACW at mid-depths. Thus, three important contact zones can be defined, SAW–NACW, SAW–MOW, and NACW–MOW, where according to previous observations (Macías et al., 2006) using *in vivo* Chla fluorescence, DCM are likely to occur. This discontinuity in the vertical composition of the DCM could be of particular relevance for the pelagic ecosystem of the Alboran Sea as the discontinuous entrance of biogeochemical material should affect the composition and behaviour of the planktonic community.

Up to date, there is no specific study aimed to analyse the relationship between chlorophyll patches and water masses and their interfaces in this oceanographic area. The highly dynamic nature of the physical structures and biological patterns in the strait means that an extensive data set is required in order to derive accurate conclusions about general trends. As tidal amplitude is *a priori* an important source of variability, it was convenient to focus the analysis on the observation of several tidal cycles.

Therefore, the main goals of this work were: (1) to determine whether an accumulation of phytoplankton cells could be observed at the different water interfaces present in the Strait of Gibraltar, (2) relate their dynamics to the stages of the tidal cycle and (3) characterise the possible differences (in composition, source and origin) of the maxima observed. Using this information, a conceptual model is developed that represents patterns of water mass circulation and biological variable distribution in relation to the tidal cycle within the strait. This model provides new information about the origin and mechanisms involved in the formation of DCMs, a subject still under debate.

2. Material and methods

Data were obtained during two simultaneous cruises in November 2003 performed in the area of the Strait of Gibraltar and western Alboran Sea on board two research vessels, B.I.O. *Hespérides* and B.O. *Mytilus*. A grid that covered the studied area (Fig. 1a) was surveyed twice at different tidal amplitudes (spring and neap tides) and wind regimes (westerlies and easterlies). From the complete grid, a set of seven stations that characterised the main hydrographic features of the strait was selected (Fig. 1b). Station 1 was used to illustrate the characteristics of the water column on the western side of the strait (region A, Fig. 1b). Station 2 described the water column on the main sill of the strait (region B, Fig. 1b). The vertical distribution of variables in the central section of

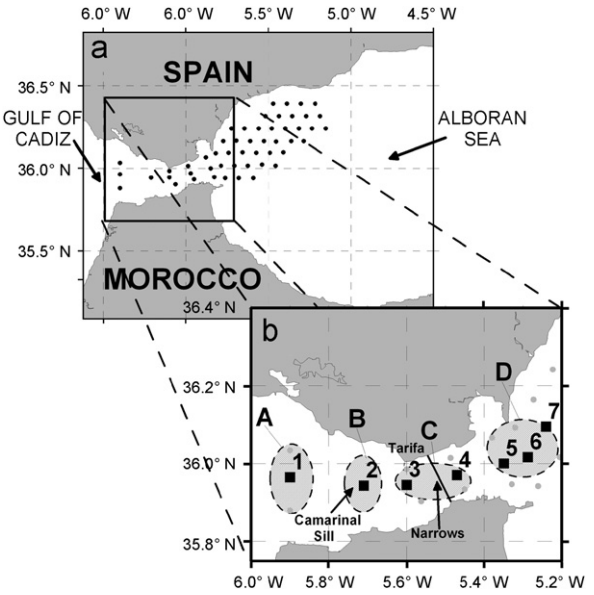

Fig. 1. (a) Grid of stations sampled in the Strait of Gibralter and NW Alboran Sea. (b) Stations selected within the main channel of the strait.

the channel (region C, Fig. 1b) was examined using the casts performed in stations 3 and 4. The description and monitoring of the eastern sector of the strait (region D, Fig. 1b) were based on data acquired at stations 5–7. Each station was sampled several times, making a total of 32 observations within the main channel of the strait.

Basic information on physical structure of the water column at each station was obtained from CTD casts. Discrete water samples were also collected at different depths to analyse several variables related to the dynamics of the pelagic ecosystem. At daytime, between 8:00 AM and 19:00 PM, photosynthetic available radiation (PAR) profiles were measured with a Satlantic PRR-600 instrument at four stations within the channel of the strait.

Total chlorophyll concentration was estimated by filtering 0.5 L of seawater through Whatman GF/F filters using the fluorometric method described by Yentsch and Menzel (1963) and modified by Holm-Hassen et al. (1965). The percentage of chlorophyll contained within cells larger than 10 μm was measured by filtering 5 L of seawater through a nylon mesh of 10 μm nominal pore diameter. The retained material was then collected by washing the mesh using a sprayer filled with clean, filtered (0.7 μm) seawater, and filtering through Whatman GF/F filters following the same protocol described above. The chlorophyll contained within cells larger than 10 μm was compared to the total chlorophyll concentration of a sample to obtain the percentage of chlorophyll attributed to larger cells.

Transparent exopolymeric particle (TEP) concentration was estimated following the colorimetric method described by Passow and Alldredge (1995) and modified by Prieto et al. (2002).

The percentage of active chlorophyll was calculated using a pulse amplitude modulated (PAM) fluorometer specifically designed to study phytoplankton cells (PhytoPAM©, see detailed description in Kolbowski and Schreiber, 1995 and in Schreiber, 1998). The PAM uses weak probe flashes to measure the change in the quantum yield of fluorescence induced by a strong pump flash. This relative change is proportional to the quantity of chlorophyll included in active phtosystem II (PS II) reaction centres as successive light pulse leads to a saturation of PS II centres and a diminution of the fluorescence quantum yield. Thus the PhytoPAM provides an estimate of the proportion of total chlorophyll within active PS II, i.e., the chlorophyll available for photosynthesis (Kolberg and Falkowski, 1993), or "active chlorophyll". Six on-board measurements of two dark-adapted replicates (previously stored in polypropylene bottles) were performed per station.

Three replicates of filtered seawater (12 mL, Whatman GF/F filters) were collected at each sampling point and stored at −20 °C for inorganic nutrient concentration determination. Concentrations of nitrate, nitrite, phosphate, silicate and ammonia were measured in the laboratory using an autoanalyser (Technicon-TRACCS 800) following the techniques of Strickland and Parsons (1972).

Analysis of pico- and nanoplankton was carried out using a flow cytometer FACSCalibur (Becton Dickinson) using two different gain settings aiming to cover the high variability of the natural phytoplankton community and red fluorescence as a threshold parameter. Acquisition time was set at 600 s and MiliQ water was used as sheath fluid. Acquisition and data analysis were carried out with the software CELL Quest™ (Becton Dickinson). Identification of *Prochlorococcus*, *Synechococcus*, small nanoplankton, large nanoplankton and *Cryptophyceae* was completed using a three-dimensional gate based on green fluorescence, red fluorescence and side scatter signal (SSC). The two prokaryotic picoplankton groups identified present a complementary distribution in the marine environment (Chisholm, 1992), as *Synechococcus* is usually more abundant in coastal regions while *Prochlorococcus* normally occurs in deeper regions of the open sea (Goericke et al., 2000; Pan et al., 2004). Differentiation between small nanoplankton (2–10 μm) and large nanoplankton (10–20 μm) was made using the size threshold defined by Rodríguez et al. (2002).

Cell abundance was transformed to carbon content (in pg C mL^{-1}) according to Heldad et al. (2003), using the ratios 0.203 and 0.031 pg C $cell^{-1}$ for *Synechococcus* and *Prochlorococcus*, respectively. For nanoplankton species, SSC signal was converted to biovolume (BV, in μm^3) using the empirical relationship shown in Eq. (1). The regression equation was obtained by measuring the BV of four different cultures of phytoplankton (measured by optic imagery) and comparing the results to the SSC signal. BV was converted to carbon using Eq. (2), proposed by Verity et al. (1992).

$$\mathrm{BV}(\mu m^3) = 0.3534 \times \mathrm{SSC} + 2.885 \quad (r^2 = 0.928; \quad n = 4; \quad p < 0.01) \tag{1}$$

$$\mathrm{pgC} = 0.433 \times \mathrm{BV}^{0.863} \quad (r^2 = 0.984) \tag{2}$$

Samples for microplankton (20–200 μm) analysis were collected using a 10 μm mesh, fixed with formalin (4–5%), and then analysed by inverted microscopy (Utermöhl, 1931, 1958).

2.1. Temporal framework and presentation of results

As tidal forcing is *a priori* one of the main elements that explains circulation dynamics in the Strait of Gibraltar, three specific periods of the tidal cycle were chosen to show the variability of water mass distribution. The selected periods were referenced to the stages of the tidal cycle recorded in the town of Tarifa, located in the middle section of the strait (Fig. 1). Thus, 2 h before high water (HW−2), 2 h after high water (HW+2) and low water (LW) were selected as periods of reference to analyse the water mass distribution and plankton patterns during the whole tidal cycle.

These stages were not selected arbitrarily, but rather on the basis of the hydrodynamics within the strait. Thus, HW−2 corresponds to the time when enhanced outflow and high current velocities over the Camarinal Sill are predicted, which can cause the generation of arrested internal waves on the sill (Bruno et al., 2002). These arrested or stationary internal waves are established over the sill 2–3 h before high water (Alonso Del Rosario et al., 2003); when the tide turns (HW), they start to move, propagating towards the Mediterranean. This is the reason why HW+2 was chosen, as it is a time when internal waves are propagating eastwards and the Atlantic flow to the Mediterranean has been re-established. The third stage (LW) corresponds to the time when the outcoming flow over the Camarinal Sill starts to increase and the internal waves nearly reach the eastern side of the strait (Farmer and Armi, 1986).

The second subsection of the results gathers together all the characteristics of the different DCMs associated with each water mass interface. For this purpose we used all the observations made during the cruise (i.e., the 32 casts).

3. Results

3.1. Tide-related variability

CTD profiles corresponding to each region within the strait at each of the selected tidal stages have been plotted together (Figs. 2–5) to allow a comparison of the tidal dynamics of water masses in each zone.

3.1.1. Region A: Atlantic sector

The TS diagram of the three casts performed in the Atlantic side of the Strait of Gibraltar during the three stages of the tidal cycle (Fig. 2a) revealed the characteristic presence of SAW, NACW and MOW. A distinctive vertical pattern was maintained throughout the tidal cycle, characterised by a superficial thermocline around 25 m between SAW and NACW and a deeper halocline situated around 150 m separating NACW and MOW (Fig. 2b).

A clear, but not very large (0.4 mg m^{-3}), chlorophyll maximum was associated with the SAW–NACW interface and strong thermocline situated at around 50–70 m. This maximum was characterised by a low percentage of chlorophyll within cells >10 μm (4–8%), low percentage of active chlorophyll (8–10%) and a relatively high TEP/Chla ratio (600–800) (Table 1).

The great similarities of the CTD cast and DCM characteristics along the tidal cycle in this area indicate that tidal forcing is not very important as a regulating factor of the hydrodynamics in this outer zone of the strait's channel.

3.1.2. Region B: Camarinal Sill

Water column composition over the Camarinal Sill was strongly dependent on the tidal cycle (Fig. 3), with a shift from a two-layer (SAW–MOW) water column in HW−2 to three-layers (SAW–NACW–MOW) during the other two stages of the tidal cycle (Fig. 3a).

When NACW was detected (HW+2 and LW), a chlorophyll maximum associated with the SAW–NACW interface (grey and dashed arrows in Fig. 3b) was found, as occurred in region A. The characteristics of this DCM were similar to those found in the western section of the strait; a low percentage of chlorophyll in cells >10 μm (9%) and low active chlorophyll (10%) (Table 1).

However, when NACW was absent (HW−2), a shallow and intense chlorophyll maximum with values >0.6 mg m^{-3} was linked to the intense thermocline and halocline associated with the SAW–MOW interface (black arrow in Fig. 3b). The main characteristics of this maximum were clearly different from the one previously described, with a considerably higher percentage of chlorophyll in cells >10 μm (20%), more active chlorophyll (60%) and a lower TEP/Chla ratio (409, Table 1).

3.1.3. Region C: central channel

Due to logistic problems, water column characteristics in the central region of the main channel were recorded only during the first tidal stage (HW−2). All three water masses (SAW, NACW and MOW) were also observed in this zone. The vertical chlorophyll profile (Fig. 4b) was characterised by two maxima situated at different depths (black arrows). The shallowest DCM, of approximately 0.5 mg m^{-3}, was observed at the SAW–NACW interface situated at 20 m, while the deeper DCM, which had lower values of chlorophyll (0.3 mg m^{-3}) was detected at the NACW–MOW interface (defined mainly by a halocline) at 50 m. The shallow maximum was similar to those found associated with the SAW–NACW interface in the rest of the region; it was characterised by a low quantity of chlorophyll in cells >10 μm (12%) and a low percentage of active chlorophyll (4%, Table 1). In contrast, the deeper maximum was characterised by a higher percentage of chlorophyll in cells >10 μm (80%), low active chlorophyll (8%) and an extremely high TEP/Chla ratio (6669, Table 1).

3.1.4. Region D: Mediterranean sector

In the eastern sector of the channel of the strait, an alternation of the composition of the water column was

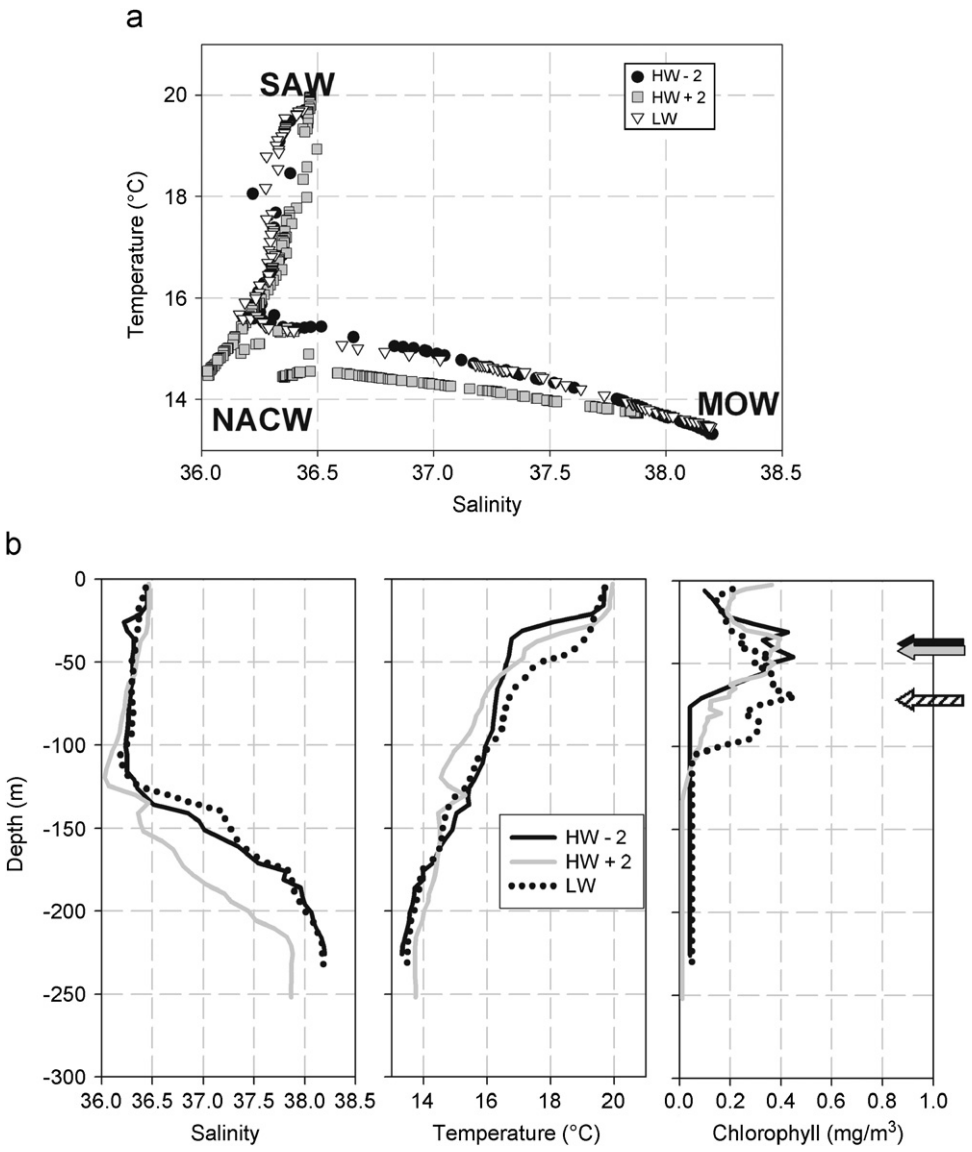

Fig. 2. TS diagrams (a) and vertical profiles (b) of the CTD casts performed in region A. Arrows mark the position of the DCM 2 h before HW (black), 2 h after HW (white) and at LW (lined).

observed again along the tidal cycle (Fig. 4a). During HW−2 and LW, only SAW and MOW were detected, while during HW+2, all three water masses were observed.

This shift in the water column composition also had effects on the vertical distribution of chlorophyll (Fig. 5b). When NACW (HW−2) was present, two maxima were detected, one at 25 m (at the SAW–NACW interface) and a second situated 75 m deep (in the NACW–MOW interface). Both DCMs were not especially intense, with the maximum values of around 0.5 mg m^{-3} being very similar to those found in region C during HW−2. When only SAW and MOW were detected (HW−2 and LW), a single chlorophyll maximum of >0.8 mg m^{-3} was observed in the upper 20 m of the water column. This maximum had a high percentage of chlorophyll in cells >10 mm (21–22%), high active chlorophyll (47–50%) and low TEP/Chla ratio (75, Table 1).

3.2. Chlorophyll maxima and water masses interfaces

At least three different types of chlorophyll maxima could be identified, each with different absolute chlorophyll values, position within the water column and physiological properties. The three types of maxima were: (i) those associated with the SAW–NACW interface, (ii) those situated between SAW and MOW and (iii) those found in the transition between NACW and MOW. The mean characteristics of each type of maximum are summarised in Fig. 6, where the confidence intervals calculated using the *t*-Student analysis (Zar, 1984) are also

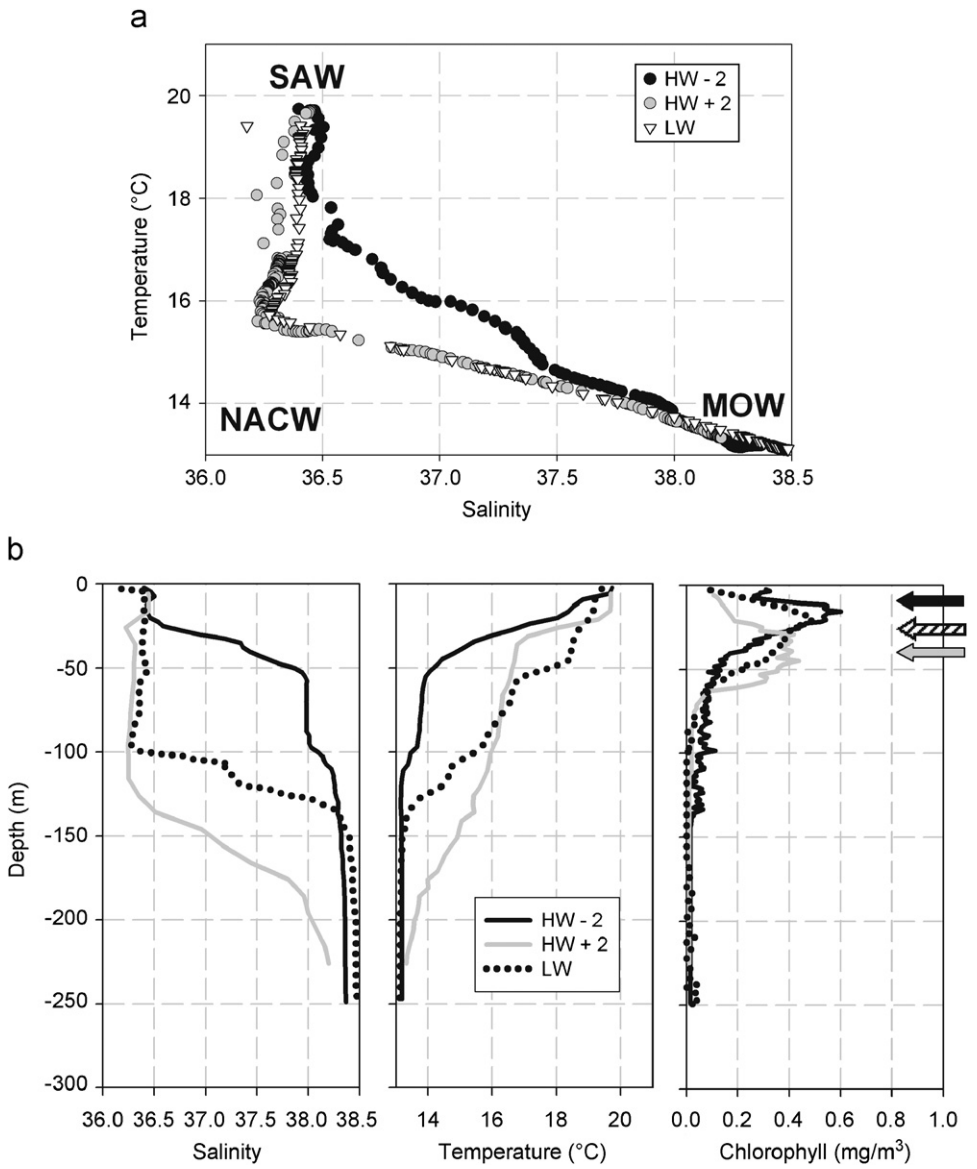

Fig. 3. TS diagrams (a) and vertical profiles (b) of the CTD casts performed in region B. Arrows mark the position of the DCM 2 h before HW (black), 2 h after HW (white) and at LW (lined).

shown. In this calculation, the 32 observations conducted within the main channel of the Strait of Gibraltar were considered.

Taking into account that the identification of the maxima was performed by considering the fluorescence profiles derived from the CTD casts, a possible explanation for these maxima could be a photoadaptation process without implying a real accumulation of phytoplankton. However, Fig. 7 shows that there is a clear relationship between chlorophyll and carbon concentration for all the identified maxima, with correlation coefficients of >0.9 ($p<0.001$) in all cases (Fig. 7, lower plate). Thus, photoadaptation does not seem to be a key factor determining the presence of the DCM, suggesting that the occurrence of the maxima could be attributable to an increase in phytoplankton biomass due to accumulation of cells at the water interfaces.

3.2.1. *Maxima between SAW and NACW*

The maxima located at the interface between SAW and NACW were specifically linked to the 26.3 isopycnal ($n=25$, coefficient of variation (CV) = 0.7%, Fig. 6b). These DCM were detected at a mean depth of 22 m ($n=25$; CV = 87%), within the photic layer ($Z_{1\%}$), which was situated at 43 m ($n=4$; CV = 14%).

The phytoplankton assemblage in these maxima was mainly composed of small cells (% chlorophyll in particles $>10\,\mu m = 12\%$, $n=25$, CV = 58%, Fig. 6d) and only 25%

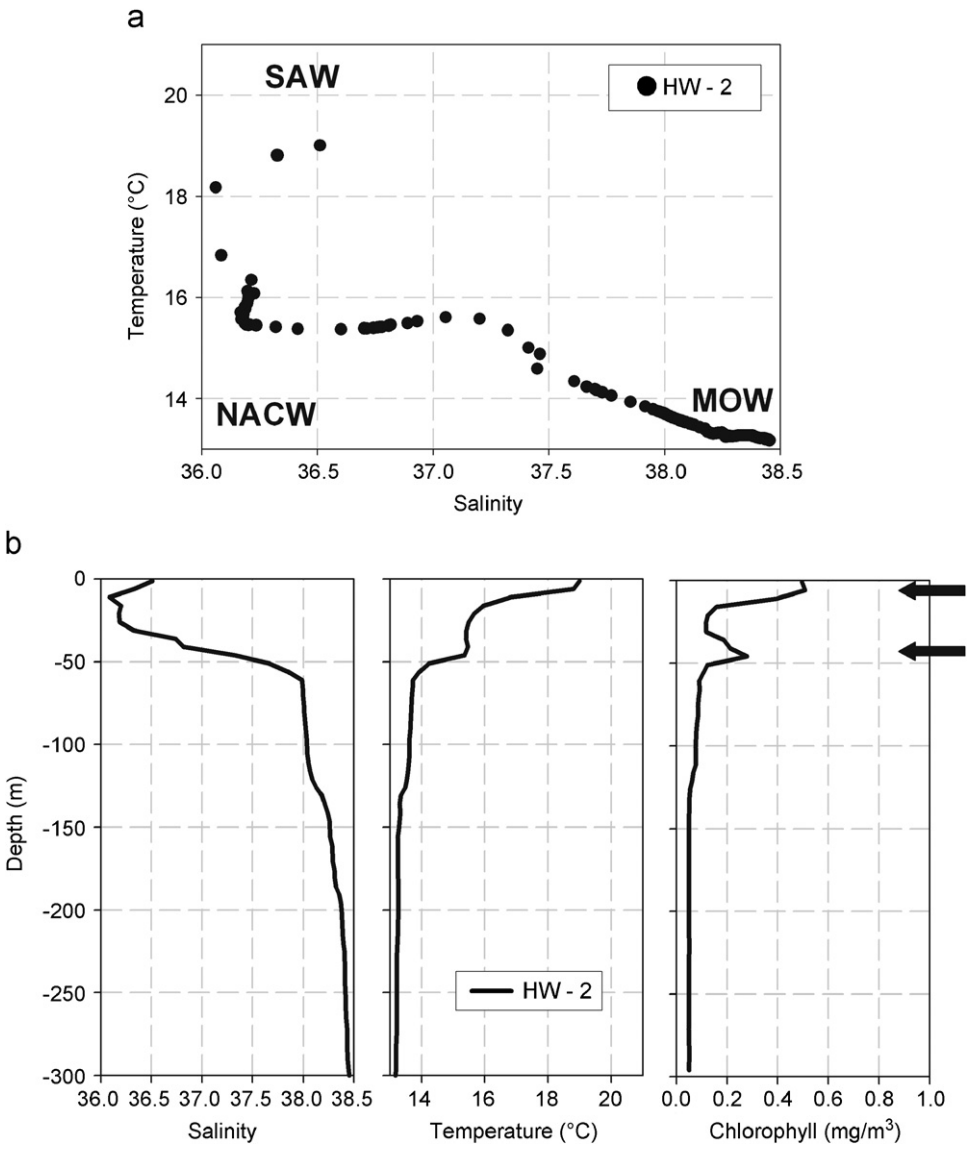

Fig. 4. TS diagrams (a) and vertical profiles (b) of the CTD casts performed in region C. Arrows mark the position of the two DCMs detected in the chlorophyll profile.

($n = 25$, CV = 60%) of the total chlorophyll was found to be photosynthetically active (Fig. 6e). Furthermore, these samples had a relatively high amount of extracellular exopolymers (mean TEP/Chla ratio = 870, $n = 25$, CV = 47%). The composition of the smallest fraction (picoplankton) of this phytoplankton assemblage was dominated by *Prochlorococcus* (mean 1346 pg C mL^{-1}; $n = 8$, CV = 12%, Fig. 8).

Light microscopy analysis revealed that the microphytoplankton fraction of these maxima consisted mainly of detritus, with only a few viable cells (data not shown).

3.2.2. Maxima between SAW and MOW

These DCMs were only present when NACW was absent, and were observed at the SAW–MOW interface on the 26.5 isopycnal ($n = 6$; CV = 0.57%, Fig. 6b). This interface was defined by the presence of both a thermocline and halocline. The mean depth where these maxima were found (20 m, $n = 6$; CV = 70%) was always lower than the calculated $Z_{1\%}$.

Mean chlorophyll concentration in these maxima was high (0.7 mg m^{-3}; $n = 6$; CV = 60%; Fig. 6b) and a large proportion was found in larger cells (around 20% of the total chlorophyll corresponded to particles $>10\,\mu m$; $n = 6$; CV = 50%). Moreover, the percentage of active chlorophyll was higher than the SAW–NACW maxima (mean = 42%; $n = 6$; CV = 64%).

Flow cytometry analysis of the samples collected in this maxima (Fig. 8) showed a decrease in the quantity of *Prochlorococcus* (mean = 671 pg C mL^{-1}; $n = 4$; CV = 20%)

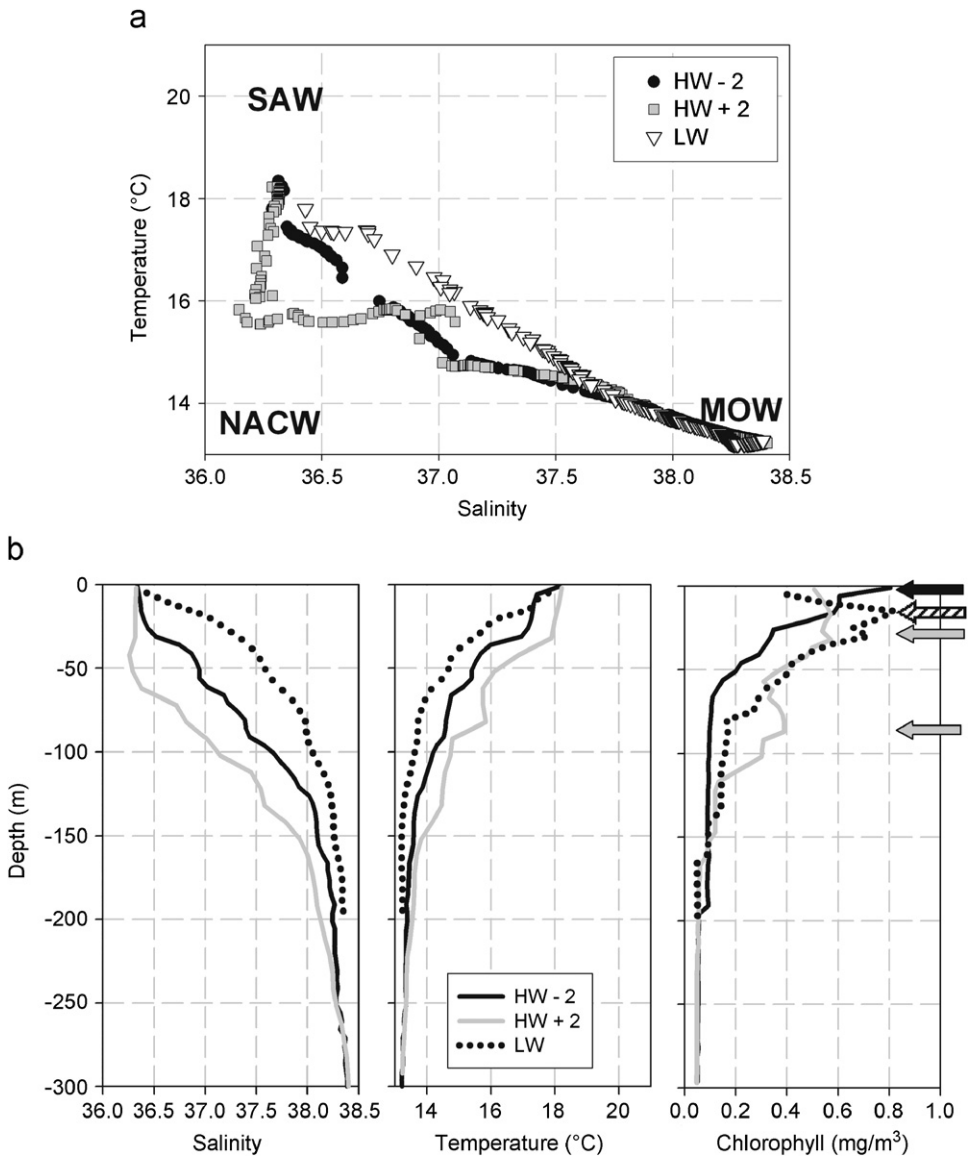

Fig. 5. TS diagrams (a) and vertical profiles (b) of the CTD casts performed in region D. Arrows mark the position of the DCM 2 h before HW (black), 2 h after HW (white) and at LW (lined).

and an increase in *Synechococcus* (mean = 1745.5 pg C mL^{-1}; $n = 4$; CV = 21%) as compared to the maxima found between SAW and NACW.

3.2.3. Maxima between NACW and MOW

These maxima were measured between the NACW and MOW water masses, at the 27.6 isopycnal ($n = 10$; CV = 0.69%). This interface was characterised by a strong halocline and a weak thermocline and was located much deeper than the others, with an average depth of 67 m ($n = 10$; CV = 27%, Fig. 6a), far below $Z_{1\%}$.

These phytoplankton patches exhibited the highest percentage of chlorophyll associated with particles $>10\,\mu m$ (mean = 30%; $n = 10$; CV = 83%), with the lowest amount of active chlorophyll (mean = 13%; $n = 10$; CV = 56%) and the highest TEP/Chla ratio (mean = 2700; $n = 10$; CV = 80%, see Fig. 7). Moreover, carbon content in pico- and nano-phytoplankton species was lower than in the other two maxima described (Fig. 8). Light microscopy analysis of the population revealed the presence of several species of diatoms (e.g. *Thalassionema nitzschioides*, *Guinardia striata*, *Coscinodiscus* sp., *Thalassiosira sp.*, *Pseudo-nitzschia* sp.) in the microplankton fraction.

4. Discussion

4.1. Origin of the identified DCM

4.1.1. Atlantic maxima (AM) between SAW and NACW

The interface between SAW and NACW is usually characterised by a strong thermocline between the surface and

Table 1
Basic attributes of the DCMs measured in each region at each tidal stage

		HW-2	HW+2	LW
Region A	Chla >10 μm (%)	4	6	8
	Chla active (%)	8	–	10
	TEP/Chla	600	625	873
Region B	Chla >10 μm (%)	20	9	9
	Chla active (%)	60	10	–
	TEP/Chla	409	563	690
Region C	Chla >10 μm (%)	12–80	–	–
	Chla active (%)	4–8	–	–
	TEP/Chla	832–6669	–	–
Region D	Chla >10 μm (%)	22	10–16	21
	Chla active (%)	47	–	50
	TEP/Chla	75	567–1371	–

When two different values appear in the same cell, two maxima were identified in a single profile.

the central waters (Gascard and Richez, 1985; Ochoa and Bray, 1991). A chlorophyll maximum linked to that shallow thermocline has been previously registered in the western section of the strait (Gómez et al., 2000; Echevarria et al., 2002; Reul et al., 2002) and in the Gulf of Cadiz (Navarro et al., 2006). Because of this, the denomination of "Atlantic maxima" (AM) was used to define this SAW–NACW chlorophyll maximum.

Navarro et al. (2006) suggested that the chlorophyll maxima associated with that interface were attributed to a functional response of the picoplankton to the existence of a nutricline between the nutrient-rich NACW and the impoverished SAW (Herbland and Voituriez, 1979). Nutrient concentration measurements in the strait during the present study support this hypothesis and the Atlantic origin of this particular DCM. Mean nitrate+nitrite (NN) concentration in the overlying waters was 0.6 μM ($n = 26$; CV = 70%), a concentration less than the threshold of 1 μM accepted as limiting for phytoplankton proliferation (Eppley et al., 1969; Wash, 1988). In contrast, NN concentration in the deeper water layer (between the 26.35 and 26.5 isopicnals) was a mean value of 2.0 μM ($n = 21$; CV = 76%), confirming the existence of a marked nutricline in this region of the water column.

The predominance of small cells in the phytoplankton assemblage of the AM (Fig. 6) is typical of oligotrophic environments (Malone, 1980; Chisholm, 1992; Li, 2002), where maxima are usually associated with gradients in nutrient distribution (Morán et al., 2001). Picoplankton composition also supports this hypothesis, as *Prochlorococcus* has been reported to be more abundant in offshore waters (Goericke et al., 2000) and is prevalent in the open region of the Gulf of Cadiz (Zabala, 1999; Reul et al., 2006).

The low percentage of active chlorophyll and the high TEP/Chla ratio (Fig. 6) of these maxima are indicative of a senescent phytoplankton population; mucilage production is known to be a good indicator of declining plankton communities (Prieto et al., 2006).

4.1.2. Suction maxima (SM) in the SAW–MOW interface

Enhanced chlorophyll maxima associated with the combined presence of a thermocline and a halocline (i.e., the SAW–MOW interface) has been previously described eastwards of the Camarinal Sill (Rodríguez et al., 1998; Gómez et al., 2000). These maxima do not seem to be linked to the presence of a nutricline, as NN concentration in the overlaying waters was around 2.2 μM ($n = 9$, CV = 53%), well above the threshold limiting value that limits phytoplankton growth. Therefore, the generation of these chlorophyll patches is likely to be related to physical processes, rather than *in situ* growth.

The higher mean concentration of chlorophyll, percentage of larger cells and active chlorophyll in these maxima would indicate a coastal origin, as larger cells are generally found in coastal environments, where nutrient inputs to the surface layer are more frequent (Malone, 1980; Mann and Lazier, 1991). Moreover, the increase in the quantity of *Synechococcus* and the decrease of *Prochlorococcus* (Fig. 8) also support the coastal origin of these chlorophyll patches as *Synechococcus* occurs mainly in shallow inshore areas (Chisholm, 1992; Goericke et al., 2000; Pan et al., 2004) and it is usually found in the coastal region of the Gulf of Cadiz (Zabala, 1999; Huertas et al., 2005; Reul et al., 2006). Also, the relatively low TEP/Chla ratio in SM is an indicator of a actively growing population as it has been documented that in early bloom stages the production of TEP is minor (Corzo et al., 2000).

These maxima appear to be linked with undulatory processes that take place in the Atlantic–Mediterranean interface (Macías et al., 2006) and, thereby, their occurrence seems to be related to the mechanisms that generate such processes. Briefly, the generation of internal waves over the Camarinal Sill is linked to the reinforcement of the outflowing Mediterranean flux occurring before the HW. At the same time, if the tidal amplitude is high enough, even the Atlantic layer reverses its movement over the Sill, flowing back to the west (Izquierdo et al., 2001). However, eastwards of the Tarifa narrows, the Atlantic layer flows to the east throughout the complete tidal cycle. These circumstances could lead to the appearance of horizontal divergences in the Atlantic layer between the Camarinal Sill and the Tarifa narrows. It has been proposed that, depending on tidal cycle's amplitude, this divergence can cause an enhanced interchange and intrusion (i.e., "suction") of coastal waters into the centre of the channel in a pulsating manner (Macías et al., 2007). Therefore, if the suggested hypothesis is valid, some chlorophyll-rich coastal waters would be incorporated into the main channel of the strait. Consequently, these chlorophyll maxima are named "suction maxima" (SM) after their probable formation mechanism. That could also explain why no NACW signal is detected when SM are present, as this water mass could not overflow the Sill against the tidal current around the HW time (see schemes in Fig. 9) being retained in the western section of the strait.

4.1.3. Deep maxima (DM) in the interface between NACW and MOW

The origin of these DM is not clear, but examination of their characteristics suggests that they are generated by

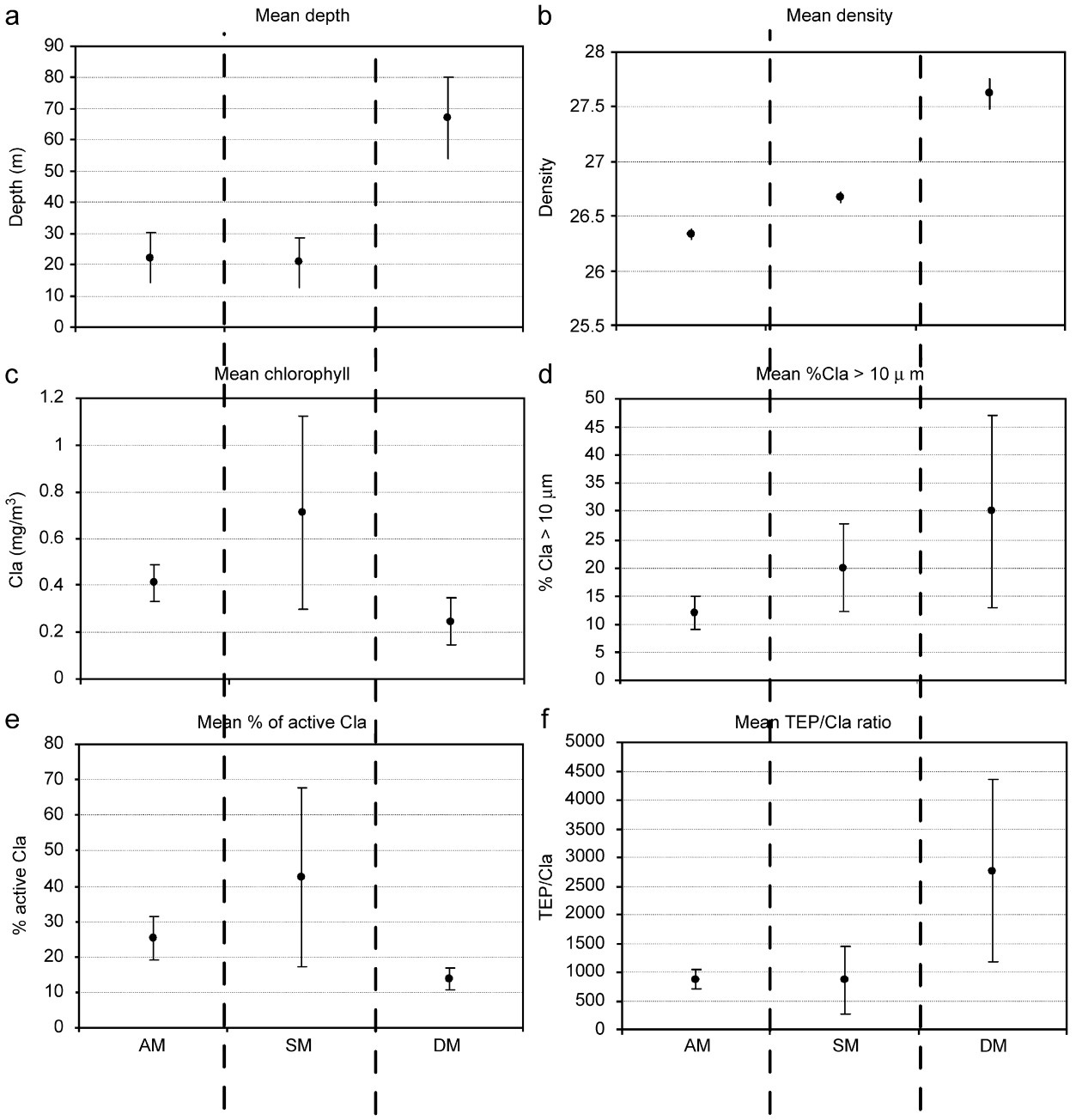

Fig. 6. Mean characteristics and 95% confidence intervals (*t*-Student analysis) of the identified maxima.

sedimentation of large aggregates (high percentage of chlorophyll in particles larger than 10 μm) formed by senescent cells (low quantity of active chlorophyll and high TEP/Chla ratio). These accumulate at the interface due to a reduction in their settling velocity caused by either the density gradient created by the strong halocline (Longhurst and Harrison, 1989; Margalef, 1989) or because of modifications in turbulence levels (Ruiz et al., 2004). The accumulation of larger particles at this interface, observed using an underwater video profiler (UVP), has been previously described by Gómez et al. (2001).

4.2. Conceptual diagrams of water mass circulation

The circulation patterns of water masses through the strait are expected to influence the position and, even, the composition of the chlorophyll maxima, so we present conceptual diagrams of water masses and DCM position during different phases of the tidal cycle in Fig. 9. Vertical

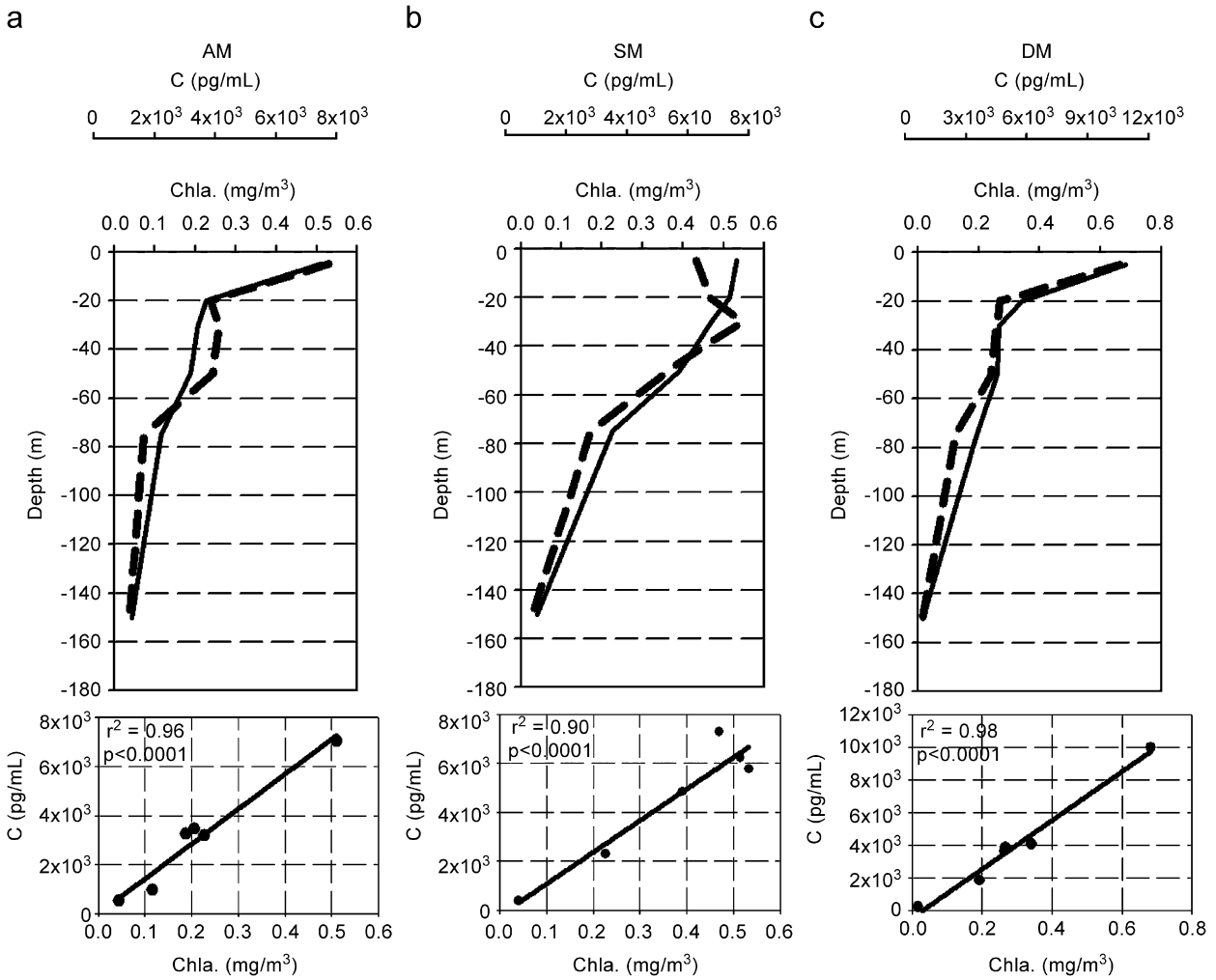

Fig. 7. Upper plate: mean vertical profiles of chlorophyll (mg m^{-3}, solid line) and carbon in pico and nannoplankton (pg C mL^{-1}, dashed line); (a) mean of stations where AM was found; (b) stations with SM presence and (c) stations where DM was located. Lower plate: scatter plot of mean C content vs. chlorophyll concentration at each sampled depth for the different maxima.

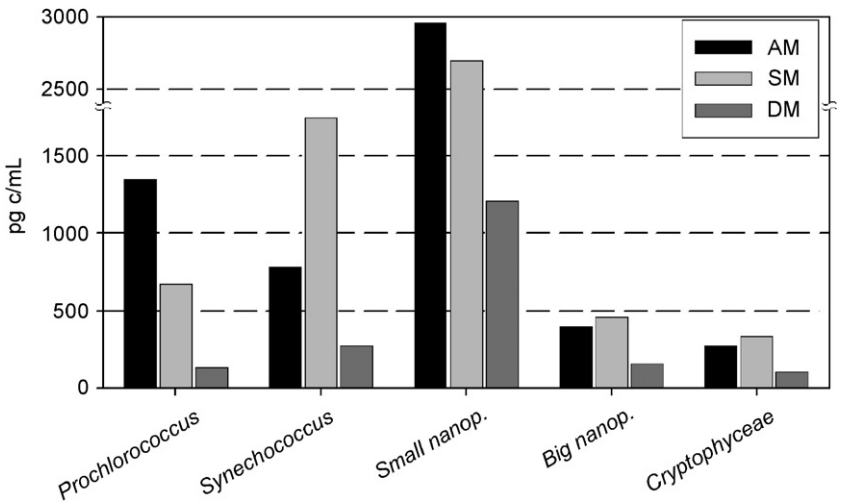

Fig. 8. Mean carbon content (pg C mL^{-1}) of the main pico- and nano-phytoplankton species in each identified maxima.

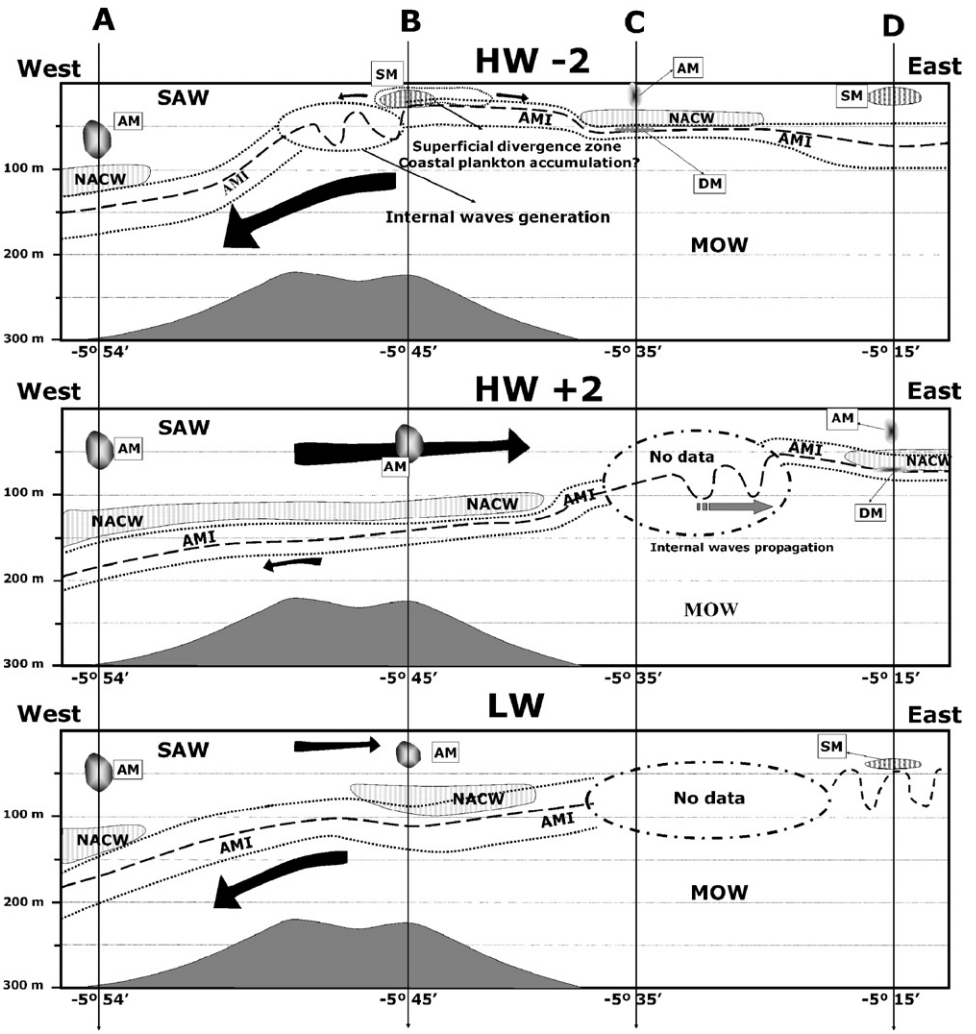

Fig. 9. Conceptual diagram showing interface and DCM positions and water mass circulation within the strait during different stages of the tidal cycle. Areas encircled by a dashed–dotted line represent values obtained from the literature (no data available). Labels indicate the names of the identified maxima according to the classification made in section 4.1.

scale maintains the original values recorded in the CTD casts (position and thickness of the interfaces and DCM) while horizontal scale has been modified to include the entire longitude of the strait.

4.2.1. Two hours before high water (HW−2)

The hydrodynamic situation during HW−2 (Fig. 9, upper plate) is normally characterised by an enhanced flow of deeper water layers over the Camarinal Sill towards the Atlantic (García-Lafuente and Vargas, 2003). When the tidal amplitude is high enough, even the upper layer can flow towards the west (La Violette and Arnone, 1988; Candela, 1990), creating a surface divergence zone over the Camarinal Sill, which is thought to be responsible for the entrainment of coastal waters into the central region of the strait (Macías et al., 2007). At this stage of the tidal cycle, internal waves have already formed (if the tidal amplitude is sufficient), but remain arrested over the Camarinal Sill because propagation against the main outflowing flow is impeded.

West of the sill (position A, Fig. 9), the vertical structure of the water column remains relatively unchanged throughout the whole tidal cycle (Fig. 2). SAW is situated in the upper 100 m of the water column, followed by NACW between 100 and 150 m and MOW at depths of <150 m. Maximum chlorophyll is observed at the SAW–NACW interface situated at 75 m (Fig. 2) and corresponds to the AM described in Section 4.1.1.

During this tidal stage, only SAW and MOW are detected over the Camarinal Sill (position B, Figs. 9 and 3), possibly due to the current regime, which prevents NACW entering this area. Surface chlorophyll maxima observed in this area are associated with the SAW–MOW interface, with the characteristics of the SM.

Towards the central region of the strait (position C, Fig. 9), the three water masses are again detected in the

water column (Fig. 4). In this situation, NACW forms a "tongue" lying over MOW and below SAW, which is located only in the central area of the strait; no NACW signal is present at positions "B" or "D" (Fig. 9). The NACW tongue may be found at intermediate depths at station "C" during this tidal stage, which originated in the previous tidal cycle when, in a situation similar to that shown in the lower plate of Fig. 9 (LW time), the NACW is able to overcome the sill after the flow eastwards is re-established, being dragged by the main surface current towards the Mediterranean side. At position "C", two chlorophyll maxima are commonly observed, an AM at the upper interface and a DM at the lower.

On the eastern side of the strait (position D, Fig. 9), only SAW and MOW are commonly observed (Fig. 5). In this area, the chlorophyll maxima linked with the interface appear to be very similar to those found over the Sill (position B), i.e., a SM.

4.2.2. Two hours after high water (HW+2)

During this phase of the tidal cycle the inflow of Atlantic water is reinforced and a weakening of the Mediterranean outflow takes place (Fig. 9, intermediate plate; Armi and Farmer, 1988). The internal waves have been already released during HW and therefore the NACW can cross the sill and flow towards the Mediterranean Sea (as shown in the CTD cast performed in position B, Fig. 3).

West of the Camarinal Sill (position A, Fig. 9), the three water masses (SAW, NACW and MOW) are commonly detected (Fig. 2) and an AM is observed at the SAW–NACW interface.

Above the Camarinal Sill (position B) the three water masses are still present, a clear NACW signal is observed between 120 and 130 m (see TS diagram and profiles in position B, Fig. 3) and an AM is still associated with the SAW–NACW interface.

During this stage of the tidal cycle the internal waves are propagating within the strait, and are expected to be around position C, probably with the SM described in position "B" of Fig. 9, upper plate (HW−2). However, there were no data available for this section of the channel during this tidal stage to confirm this assumption.

At position "D", the tongue of NACW described in region "C" of Fig. 9, upper plate was also detected. Furthermore, the two maxima linked to the interfaces SAW–NACW and NACW–MOW were again clearly observed in the CTD profile (Fig. 5).

4.2.3. Low water (LW)

During LW, the internal waves are expected to be close to the eastern side of the strait (Farmer and Armi, 1986; Macías et al., 2006). At this stage, the current velocity of the surface layer over the sill progressively decreases and the deeper outflow reinforces. In this situation, a shallowing of the AMI takes place, obstructing the eastwards flow of NACW (Fig. 9, lower plate).

As previously indicated, in position "A" (west of the sill), the composition of the water column is very similar to that described in the two previous diagrams (Fig. 2), i.e., the presence of all three water masses and an AM at the upper interface.

The signature of NACW was still detectable in the profiles performed over the Camarinal Sill (position B, Fig. 3). Four hours later, NACW forms the tongue described in position "C" at HW−2 (Fig. 9, upper plate). An AM was registered between the SAW and the NACW.

During this phase of the tidal cycle, the internal waves generated in the previous outflowing event are expected to be approaching the eastern side of the strait (position D). In the cast performed at this position there was no NACW signal and a shallow SM connected to the SAW–MOW interface was observed (Fig. 5). This maximum was very similar to the DCM associated with the generation of internal waves located over the Camarinal Sill at HW−2 (position B, Fig. 9, upper plate). Completing the tidal cycle and 4 h after the situation above, the scenario was again comparable to the one described in the upper plate of Fig. 9.

4.3. Chlorophyll maxima in the strait

This work clearly shows how the same biological feature (i.e., a DCM linked to water mass interfaces) in a particular oceanographic area can be due to a number of different factors; *in situ* growth, physical accumulation or advection. Therefore, in order to assess the origin and formation mechanisms of DCMs, a thorough understanding of physical and biological forcing is essential.

The conceptual model presented to explain the nature of the DCM observed in the Strait of Gibraltar is strongly influenced by both tidal amplitude and the wind regime. It is well established that tidal amplitude strongly influences the dynamics of currents over the Camarinal Sill, changing the quantity and periodicity of inputs of NACW into the Atlantic jet (Macías et al., 2006). In addition, the zonal wind direction and intensity could affect the dynamics of water masses (Gómez et al., 2004).

Therefore, a discontinuous entrance of different phytoplankton assemblages into the Alboran Sea would be expected. In fact, recent observations of the composition of the Atlantic jet (Macías et al., 2006) have shown a clear relationship between the absence of NACW signal and the highest levels of chlorophyll in the eastern section of the strait. These observations gathered together more than 140 profiles of the vertical structure of the Atlantic jet crossing the strait during nine different tidal cycles, under diverse meteorological conditions and covering several periods of the year. The analysis of this extensive data set has shown a very regular increase in the chlorophyll concentration (average chlorophyll increase of 28%) of the water column when NACW was absent, regardless of the tidal stage and meteorological conditions. It was also possible to distinguish the different maxima identified in this work, with the maximum chlorophyll content corresponding to SM (always in the absence of NACW signal in the water column); a lower concentration in the presence of NACW (corresponding to AM) and the deep maximum in the NACW and MOW transition zone. Hence, the patterns highlighted in the present study are maintained annually and are a representative description of the typical patterns of circulation through the strait.

Also, a recently developed physical–biological coupled model of the channel of the strait (Macías et al., 2007) has shown that the high chlorophyll patches consistently detected in the eastern sector of the strait (the SM presented in this work) cannot be explained only by *in situ* growth of the phytoplankton while crossing the strait, as the average residence time in the channel is not long enough to allow noticeable growth. Furthermore, dilution effects due to mixing would prevail, impeding phytoplankton proliferation. In this sense, the present work adds new elements that support the hypothesis that some of these pulsating chlorophyll patches (the so-called SM) could have a coastal origin through lateral advection and mixing.

This discontinuous entrance of biogeochemical material through the strait is important for the pelagic ecosystem of the Alboran Sea, as a pulsating input of both plankton and nutrients could drive the behaviour of the system. Therefore, the nature of this input should be taken into account when explaining the spatial and temporal patterns of biogeochemical elements in the Alboran basin. For example, Ruiz et al. (2001) linked chlorophyll maxima that gradually became more intense towards the east of the basin with the presence of nutrient enriched surface layers by NACW injection.

Furthermore, as the strait is the sole connexion between the Mediterranean Sea and the open Atlantic Ocean, understanding of the specific mechanisms of biogeochemical interchanges is extremely important for assessing the element budget of this semi-enclosed basin.

In summary, tide-induced variability within the Strait of Gibraltar not only affects the transport and circulation of the water masses that meet in the area, but also the distribution and characteristics of chlorophyll patches. This fact corroborates the importance of tide-induced phenomena in explaining physical and biological structures at the regional scale. In the future, special attention must be paid for understanding the mechanisms (and their variability) controlling the interchange between coastal areas and the centre of the channel. Specific research cruises with the necessary spatial–temporal resolution to resolve these relatively fast processes, as well as accurate two-dimensional models, are required to study these phenomena, especially in the nearest shallow coastal areas, which have a high chlorophyll concentration and higher residence time, and in those areas where interchanges (such as the Tarifa–Camarinal Sill region) are likely (Izquierdo et al., 2001).

Acknowledgements

This work was funded by the Spanish National Research Program, Projects; REN-2001-2733-C02-02 and CTM2005-08142-C03-01. D.M. was supported by a grant from the Spanish FPI fellowship program. We thank S. Rivas and E.P. Morris for correcting the English language of the text.

References

Alonso Del Rosario, J.J., Bruno, M., Vázquez, A., 2003. The influence of tidal hydrodynamic conditions on the generation of lee waves at the main sill of the Strait of Gibraltar. Deep-Sea Research I 50, 1005–1021.

Armi, L., Farmer, D., 1985. The internal hydraulics of the Strait of Gibraltar and associated sill and narrows. Oceanologica Acta 8 (1), 37–46.

Armi, L., Farmer, D., 1988. The flow of Mediterranean Water through the Strait of Gibraltar. Progress in Oceanography 21, 41–82.

Béthoux, J.P., 1979. Budgets of the Mediterranean Sea, their dependence on local climate and on the characteristics of the Atlantic waters. Oceanologica Acta 2, 137–163.

Boyce, F.M., 1975. Internal waves in the Strait of Gibraltar. Deep-Sea Research 22, 597–610.

Bray, N.A., Ochoa, J., Kinder, T.H., 1995. The role of interface in exchange through the Strait of Gibraltar. Journal of Geophysical Research 100 (C6), 10755–10776.

Bruno, M., Alonso, J.J., Cózar, A., Vidal, J., Ruiz-Cañavate, A., Echevarría, F., Ruiz, J., 2002. The boiling-water phenomena at Camarinal Sill, the Strait of Gibraltar. Deep-Sea Research II 49, 4097–4113.

Candela, J., 1990. The Barotrophic Tide in the Strait of Gibraltar. The Physical Oceanography of Sea Straits. Kluwer Academic Publishers, Dordrecht, The Netherlands, pp. 457–475.

Chisholm, S.W., 1992. Phytoplankton size. In: Falkowski, P.G., Woodhead, A.D. (Eds.), Primary Productivity and Biogeochemical Cycles in the SEA. Plenum Press, New York, pp. 213–223.

Corzo, A., Morillo, J.A., Rodríguez, S., 2000. Production of transparent exopolymer particles (TEP) in cultures of Chaetoceros calcitrans under nitrogen limitation. Aquatic Microbial Ecology 23, 63–72.

Cullen, J.J., Eppley, R.W., 1981. Chlorophyll maximum layers of the southern California Bight and possible mechanisms of their formation and maintenance. Oceanologica Acta 4, 23–32.

Echevarria, F., García-Lafuente, J., Bruno, M., Gorsky, G., Goutx, M., González, N., García, C.M., Gómez, F., Vargas, J.M., Picheral, M., Striby, L., Varela, M., Alonso, J.J., Reul, A., Cózar, A., Prieto, L., Sarhan, T., Plaza, F., Jiménez-Gómez, F., 2002. Physical–biological coupling in the Strait of Gibraltar. Deep-Sea Research II 49, 4115–4130.

Eppley, R.W., Rogers, J.N., McCarthy, J.J., 1969. Half saturation constants for uptake of nitrate and ammonium by marine phytoplankton. Limnology and Oceanogaphy 14, 912–920.

Estrada, M., Marrase, C., Latasa, M., Berdalet, E., Delgado, M., Riera, T., 1993. Variability of the Deep Chlorophyll Maximum characteristics in the northwestern Mediterranean. Marine Ecology Progress Series 92 (3), 289–300.

Estrada, M., Varela, R.A., Salat, J., Cruzado, A., Arias, E., 1999. Spatio-temporal variability of the winter phytoplankton distribution across the Catalan and North Balearic fronts (NW Mediterranean). Journal of Plankton Research 21 (1), 1–20.

Farmer, D., Armi, L., 1986. Maximal two-layer exchange over a sill and through the combination of a sill and contraction with barotropic flow. Journal of Fluid Mechanics 164, 53–76.

García-Lafuente, J., Vargas, J.M., 2003. Recent observations of the exchanged flows through the Strait of Gibraltar and their fluctuations at different time scales. Recent Research Development in Geophysics 5, 73–84.

Gascard, J.C., Richez, C., 1985. Water masses and circulation in the Western Alboran Sea and in the Straits of Gibraltar. Progress in Oceanography 15, 157–216.

Goericke, R., Olson, R.J., Shalapyonok, A., 2000. A novel niche for *Phroclorococcus* sp. in low light suboxic environments in the Arabian Sea and the Eastern Tropical North Atlantic. Deep-Sea Research I 47, 1183–1205.

Gómez, F., Echevarría, F., García, C.M., Prieto, L., Ruíz, J., Reul, A., Jiménez-Gómez, F., Varela, M., 2000. Microplankton distribution in the Strait of Gibraltar, coupling between organism and hydrodynamics structures. Journal of Plankton Research 22 (4), 603–617.

Gómez, F., Gorsky, G., Striby, L., Vargas, J.M., Gónzalez, N., Picheral, M., García-Lafuente, J., Varela, M., Goutx, M., 2001. Small-scale temporal variations in biogeochemical features in the Strait of Gibraltar, Mediterranean side—the role of NACW and the interface oscillation. Journal of Marine Systems 30, 207–220.

Gómez, F., Gorsky, G., García-Górriz, E., Picheral, M., 2004. Control of the phytoplankton distribution in the Strait of Gibraltar by wind and fortnightly tides. Estuarine Coastal and Shelf Science 59, 485–497.

Gran, H.H., 1931. On the conditions for the production of plankton in the sea. Raap. P.-v Réun. Conseil International pour l'Exploration de la Mer 75, 37–46.

Guibout, P., 1987. Atlas Hydrologique de la Mediterranee. Lab. D'Ocean. Phys. du Mus. d'Historie Nat., Paris.

Heldad, M., Sacanlan, D.J., Norlan, S., Thingstad, F., Mann, N.H., 2003. Elemental composition of single cells of various strains of marine

Prochlorococcus and *Synechococcus* using X-ray microanalysis. Limnology and Oceanography 48 (5), 1732–1743.
Herbland, A., Voituriez, B., 1979. Hydrological structure analysis for estimating the primary production in the tropical Atlantic Ocean. Journal of Marine Research 37, 87–101.
Holm-Hassen, O., Lorenzen, C.J., Homes, R.W., Strickland, J.D.H., 1965. Fluorometric determination of chlorophyll. Journal du Conseil International pour l'Exploration de la Mer 187, 9–18.
Huertas, E., Navarro, G., Rodríguez-Gálvez, S., Prieto, L., 2005. The influence of phytoplankton biomass on the spatial distribution of carbon dioxide in surface sea water of a coastal area of the Gulf of Cádiz (southwestern Spain). Canadian Journal of Botany 83, 929–940.
Izquierdo, A., Tejedor, L., Sein, D.V., Backhaus, J.O., Brandt, P., Rubino, A., Kagan, B.A., 2001. Control variability and internal bore evolution in the Strait of Gibraltar: a 2-D two-layer model study. Estuarine, Coastal and Shelf Science 53, 637–651.
Jamart, B.M., Winter, D.F., Banse, K., Anderson, G.C., Lam, R.K., 1977. A theoretical study of phytoplankton growth and nutrient distribution in the Pacific Ocean off the northwestern US coast. Deep-Sea Research 24, 733–753.
Kolberg, Z., Falkowski, P.G., 1993. Use of active fluorescence to estimate phytoplankton photosynthesis in situ. Limnology and Oceanography 38 (8), 1646–1665.
Kolbowski, J., Schreiber, U., 1995. Computer-controlled phytoplankton analyzer based on a 4-wavelengths PAM chlorophyll fluorometer. In: Mathis, V.P. (Ed.), Photosynthesis, From Light to Biosphere. Kluwer Academic Publishers, Dordrecht, The Netherlands, pp. 825–828.
La Violette, P.E., 1995. Seasonal and interannual variability of the western Mediterranean Sea. In: Coastal and Estuarine Studies, vol. 46. American Geophysical Union Edition.
La Violette, P.E., Arnone, R.A., 1988. A tide-generated internal waveform in the western approaches to the Strait of Gibraltar. Journal of Geophysical Research 93 (C12), 15653–15667.
Li, W.K.W., 2002. Macroecological patterns of phytoplankton in the northwestern North Atlantic Ocean. Nature 419, 154–157.
Longhurst, A., Harrison, A., 1989. The biological pump, profiles of plankton production and consumption in the upper ocean. Progress in Oceanography 22, 47–123.
Macías, D., García, C.M., Echevarría, F., Vázquez, A., Bruno, M., 2006. Tidal induced variability of mixing processes on Camarinal Sill, Strait of Gibraltar. A pulsating event. Journal of Marine Systems 60, 177–192.
Macías, D., Martin, A.P., García, C.M., Bruno, M., García Lafuente, J., Izquierdo, A., Vázquez, A., Yool, A., Sein, D., Echevarría, F., 2007. Mixing and biogeochemical effects induced by tides on the Atlantic–Mediterranean flow in the Strait of Gibraltar. An analysis through a physical–biological coupled model. Progress in Oceanography 74, 252–272.
Malone, T.C., 1980. Algal size. In: Morris, I. (Ed.), The Physiological Ecology of Phytoplankton. Blackwell Scientific Publications, Oxford, pp. 133–463.
Mann, K.H., Lazier, J.R.N., 1991. Dynamics of marine ecosystems. In: Biological–Physical Interactions in the Oceans. Blackwell Scientific Publications, Oxford.
Margalef, R., 1978. Life-forms of phytoplankton as survival alternatives in an unstable environment. Oceanologica Acta 1, 493–509.
Margalef, R., 1989. Ecología. Ediciones Omega.
Morán, X.A.G., Taupier-Letage, I., Vázquez-Dominguez, E., Ruiz, S., Arin, L., Raimbault, P., Estrada, M., 2001. Physical–biological coupling in Algerian Basin (SW Mediterranean): influence of mesoscales instabilities on the biomass and production of phytoplankton and bacterioplankton. Deep-Sea Research I 48, 405–437.
Navarro, G., Ruiz, J., Huertas, I.E., García, C.M., Criado-Aldeanueva, F., Echevarría, F., 2006. Basin scale structures governing the position of the subsurface chl maximum in the gulf of Cádiz. Deep-Sea Research II 53, 1461–1481.
Ochoa, J., Bray, N.A., 1991. Water mass exchange in the Gulf of Cadiz. Deep-Sea Research 38 (1), S465–S503.
Pan, L.A., Zhang, L.H., Zhang, J., Gasol, J.M., Chao, M., 2004. On board flow cytometry observations of picoplankton comunity structure in the East China Sea during the fall of different years. FEMS Microbiology Ecology.
Passow, U., Alldredge, A.L., 1995. A dye-binding assay for the spectrophotometric measurement of transparent exopolymer particles TEP. Limnology and Oceanography 40 (7), 1326–1335.
Prieto, L., Ruiz, J., Echevarría, F., García, C.M., Bartual, A., Gálvez, J.A., Corzo, A., Macías, D., 2002. Scales and processes in the aggregation of diatom blooms, high time resolution and wide size range records in a mesocosm study. Deep-Sea Research I 49, 1233–1253.
Prieto, L., Navarro, G., Cózar, A., Echevarría, F., García, C.M., 2006. Distribution of TEP in the euphotic and upper mesopelagic zones of the southern Iberian coasts. Deep-Sea Research II 53, 1314–1328.
Reul, A., Vargas, J.M., Jiménez-Gómez, F., Echevarría, F., García-Lafuente, J., Rodríguez, J., 2002. Exchange of planktonic biomass through the Strait of Gibraltar in late summer conditions. Deep-Sea Research II 49, 4131–4144.
Reul, A., Muñoz, M., Criado-Aldeanueva, F., Rodríguez, V., 2006. Spatial distribution of phytoplankton $<13\,\mu m$ in the Gulf of Cádiz in relation to water masses and circulation pattern under westerly and easterly wind regimes. Deep-Sea Research II 53, 1294–1313.
Rodríguez, J., Blanco, J.M., Jiménez-Gómez, F., Echevarría, F., Gil, J., Rodríguez, V., Ruiz, J., Bautista, B., Guerrero, F., 1998. Patterns in the size structure of the phytoplankton community in the deep fluorescence maximum of the Alboran Sea southwestern Mediterranean. Deep-Sea Research I 45, 1577–1593.
Rodríguez, J., Jiménez-Gómez, F., Blanco, J.M., López-Figueroa, F., 2002. Physical gradients, and spatial variability of the size structure and composition of phytoplankton in the Gerlache Strait (Antarctica). Deep-Sea Research II 49, 693–706.
Ruiz, J., Echevarría, F., Font, J., Ruiz, S., García, E., Blanco, J.M., Jiménez-Gómez, F., Prieto, L., González-Alaminos, A., García, C.M., Cipollini, P., Snaith, H., Bartual, A., Reul, A., Rodríguez, V., 2001. Surface distribution of chl, particles and gelbstoff in the Atlantic jet of the Alborán Sea, from submesoscale to subinertial scales of variability. Journal of Marine Systems 29, 277–292.
Ruiz, J., Macías, D., Peters, F., 2004. Turbulence increases the average settling velocity of phytoplankton cells. Proceedings of the National Academy of Sciences of USA 101 (51), 17720–17724.
Schreiber, U., 1998. Chlorophyll fluorescence, new instruments for new applications. In: Garab, V.G. (Ed.), Photosynthesis, Mechanisms and Effects. Kluwer Academic Publishers, Dordrecht, The Netherlands, pp. 4253–4258.
Strickland, J.D.H., Parsons, T.R., 1972. A practical handbook of seawater analysis, second ed. In: Bulletin of Fisheries Research Board of Canada, vol. 167, pp. 1–310.
Sverdrup, H.U., 1953. On conditions for the vernal blooming of phytoplankton. Journal du Conseil Permanante International pour l'Exploration de la Mer 18, 287–295.
Taguchi, S., Ditullio, G.R., Laws, E.A., 1984. Physiological characteristics and production of mixed layer and chl maximum phytoplankton populations in the Caribbean Sea and western Atlantic Ocean. Deep-Sea Research 35, 1363–1377.
Utermöhl, H., 1931. Neue Wege in der quantitaven Erfassung des Planktons. Internationale Vereinigung für Theoretische und Angewandte Limnologie Verhandlungen 5 (2), 567–597.
Utermöhl, H., 1958. Zur Vervollkommnung der quantitativen Phytoplankton-Methodik. Internationale Vereinigung fur Limnologie, Mitteilungen 9, 1–38.
Verity, P., Robertson, G., Tronzo, C., Andrews, M., Nelson, R., 1992. Relationships between cell volume and the carbon and nitrogen content of marine photosynthetic nanoplankton. Limnology and Oceanography 37 (7), 1434–1446.
Wash, J.J., 1988. On the Nature of Continental Shelves. Academic Press, New York, p. 126.
Wesson, J.C., Gregg, M.C., 1994. Mixing at Camarinal Sill in the Strait of Gibraltar. Journal of Geophysical Research 99 (C5), 9847–9878.
Yentsch, C.S., Menzel, D.W., 1963. A method for the determination of phytoplankton chl and phaeophytin by fluorescence. Deep-Sea Research 21, 1191–1218.
Zabala, L., 1999. Estudio del Picoplancton Autótrofo en el Golfo de Cádiz y Mar de Alborán Mediante Citometría de Flujo. Departamento de Biología, Universidad de Cádiz, Cádiz.
Zar, J.H., 1974. Biostatistical Analysis. Prentice Hall International Editions, Englewood Cliffs, NJ, 265pp.